

On 2.7 μm Emission from Er-doped Large Bandgap Hosts

H. Vrielinck^{1,2}, I. Izeddin¹, V.Y. Ivanov^{1,3}, T. Gregorkiewicz¹, F. Callens², D. S. Lee⁴, A. J. Steckl⁴ and N. M. Khaidukov⁵

¹ Van der Waals-Zeeman Institute, University of Amsterdam, Valckenierstraat 65, NL-1018XE, Amsterdam, The Netherlands

² Department of Solid State Sciences, Ghent University Krijgslaan 281-S1, B-9000 Gent, Belgium

³ Institute of Physics, Polish Academy of Sciences, Lotnikow 32-46, PL-02668 Warsaw, Poland

⁴ Nanoelectronics Laboratory, University of Cincinnati, Cincinnati, OH 45221-0030, United States

⁵ Institute of General and Inorganic Chemistry, Russian Academy of Sciences, Leninskii Prospect, 119991 Moscow, Russian Federation.

ABSTRACT

The potential of Er-doped Cs_2NaYF_6 and GaN for mid-infrared emission at $\lambda \approx 2.7 \mu\text{m}$ is investigated using time-resolved optical spectroscopy. This emission results from electronic transitions between the second (${}^4I_{11/2}$) and first (${}^4I_{13/2}$) excited states of the Er^{3+} ion. By recording the photoluminescence transients for the ${}^4I_{11/2} \rightarrow {}^4I_{15/2}$ and ${}^4I_{13/2} \rightarrow {}^4I_{15/2}$ transitions after pulsed excitation, we determine the lifetime of the ${}^4I_{11/2}$ level and demonstrate that the ${}^4I_{13/2}$ state is populated from this level. Our results indicate that both host lattices should enable 2.7 μm emission, which is temperature-stable but subject to concentration quenching.

INTRODUCTION

Mid-infrared (MIR) laser radiation in the 2 – 3 μm range has applications in the fields of remote sensing, trace gas monitoring, and laser surgery [1]. Currently, optically (flashlamp or diode) pumped rare-earth (RE) -doped insulating inorganic crystals or glasses are used as laser sources in this range [2]. Especially for laser surgery applications, research towards tunable and more compact, electrically pumped sources is still ongoing. In the past few years, $\text{ZnSe}:\text{Cr}^{2+}$ has emerged as widely tunable laser medium, covering the complete 2 – 3 μm range, but electrical pumping of such crystals is yet to be demonstrated [1,3]. The design of more compact MIR lasers has focused towards diode-pumped fiber lasers [4]. However, electrically pumped media, preferably compatible with Si technology, would result in even cheaper and more compact sources. Visible electroluminescence (EL) from RE doped hexagonal GaN, epitaxially grown on Si substrates, has already been demonstrated several years ago [5]. Recently, a CMOS-compatible spin coating technique for GaN powders on Si has been developed and green luminescence has been obtained from Er-doped powders [6]. As the intra-4f transition between the second (${}^4I_{11/2}$) and first (${}^4I_{13/2}$) excited states of the Er^{3+} ion is in the range of interest (2.7 – 3.0 μm , depending on the host), it is interesting to explore the potential of Er-doped GaN as active MIR lasing medium.

In the present work, we address temporal aspects of the ${}^4I_{11/2} \rightarrow {}^4I_{13/2}$ transition of Er^{3+} in GaN, as well as possible luminescence quenching mechanisms. To this end, the kinetics of photoluminescence (PL) for the ${}^4I_{11/2} \rightarrow {}^4I_{15/2}$ transition at $\lambda \approx 1.0 \mu\text{m}$ and the ${}^4I_{13/2} \rightarrow {}^4I_{15/2}$

transition at $\lambda \approx 1.5 \mu\text{m}$ are studied. We hereby take advantage of the highly sensitive and fast detectors, developed for this wavelength range. Meanwhile, special precautions, to be taken when directly detecting radiation with $\lambda > 2.5 \mu\text{m}$ in order to prevent absorption by air (water) and commonly used silica lenses, are avoided. In a similar way, we have also studied Er^{3+} -doped Cs_2NaYF_6 . In this crystal Er^{3+} can only be incorporated on Y^{3+} positions, which have O_h point group symmetry and are widely spaced (nearest neighbor distance 0.64 nm [7]). As these crystals accept Er-concentrations up to 100 % (all Y^{3+} ions substituted), they present a good model system for investigating the influence of Er-concentration on the $2.7 \mu\text{m}$ emission.

EXPERIMENTAL DETAILS

The $\text{Cs}_2\text{NaY}_{1-x}\text{Er}_x\text{F}_6$ crystals ($x = 0.001, 0.01, 0.1, \text{ and } 1$) were hydrothermally grown, using Er_2O_3 as dopant [8]. The hexagonal $\text{GaN}:\text{Er}^{3+}$ samples were epitaxially grown on a p -type (111) Si substrate, after deposition of an AlN buffer layer, using the solid source molecular beam epitaxy method [9]. The Er-concentration in these samples is estimated at 1 at. %.

Time-resolved (TR) PL measurements were performed using a Nd:YAG-pumped optical parametric oscillator as tunable pulsed laser excitation source, generating 5 ns wide pulses, with a maximum energy of 1 mJ, at a repetition rate of 10 Hz in the $\lambda = 410 - 2200 \text{ nm}$ range. For measurements at low temperature, the GaN samples, which exhibit good thermal conductivity, were placed in a closed-cycle cryostat, with a minimum operation temperature $\sim 20 \text{ K}$, whereas for the poorly conducting Cs_2NaYF_6 crystals a He flow cryostat was used. The luminescence light was dispersed with a 1 m monochromator and detected with a liquid N_2 -cooled InGaAs photomultiplier (300 – 1700 nm). For the slow kinetics in Cs_2NaYF_6 the excitation repetition rate was lowered by blocking laser pulses with a shutter. The detector was operated in photon counting mode for detecting the much faster kinetics of Er^{3+} in GaN.

EXPERIMENTAL RESULTS AND DISCUSSION

In Fig. 1 the TR PL for the ${}^4I_{11/2} \rightarrow {}^4I_{15/2}$ and ${}^4I_{13/2} \rightarrow {}^4I_{15/2}$ transitions in a 1 % Er^{3+} -doped Cs_2NaYF_6 crystal ($x = 0.01$), measured at 4.2 K, is shown. In view of the large average dopant ion spacing at this concentration, only limited effects of interactions and energy migration between Er^{3+} ions are expected. The PL transients are analyzed assuming first order decay kinetics in an atomic three levels system (see excitation schemes in Fig. 1), leading to

$$I_{\text{PL}}(t) = A (e^{-t/\tau_d} - e^{-t/\tau_r}) , \quad (1)$$

where τ_r and τ_d represent the rise and decay times of the signal, respectively, which correspond to the population time and lifetime of the upper level involved in the detected luminescence transition. Traces (a) and (b) are recorded after exciting the Er^{3+} ions to the ${}^2H_{11/2}$ level, which presents the highest excitation efficiency for $1.54 \mu\text{m}$ emission. The TR PL from the second excited state is perfectly reproduced assuming a rise time of 0.5 ms and a decay time of 21 ms. Although in principle several relaxation paths from the ${}^2H_{11/2}$ to the ${}^4I_{13/2}$ are possible, the kinetics of luminescence from the first excited state show a single rise time of 21 ms and a decay time of 100 ms. These results indicate that the lifetimes of the second and first excited states of Er^{3+} in Cs_2NaYF_6 are 21 and 100 ms, respectively, and that the ${}^4I_{13/2}$ state is (nearly) exclusively

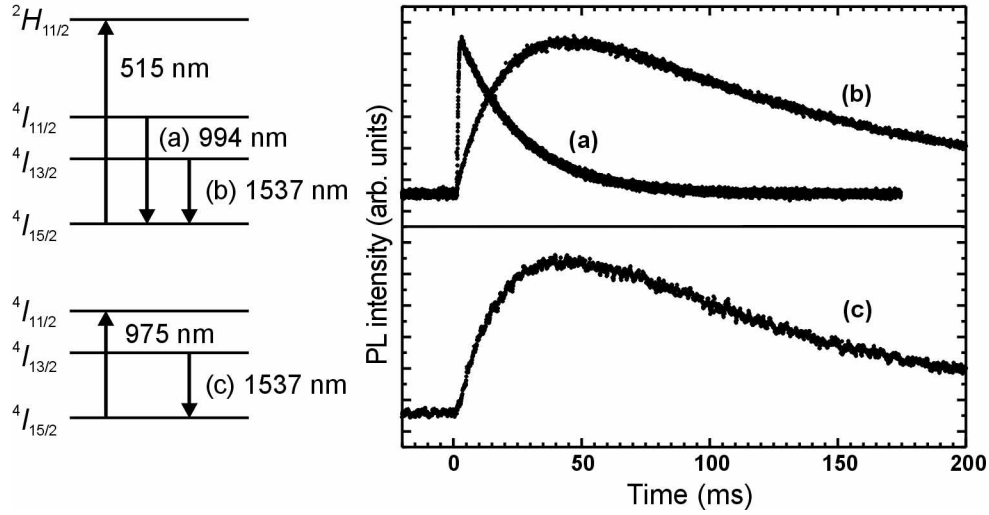


Figure 1 : Time resolved PL of the transitions from the second and first excited states of Er^{3+} in $\text{Cs}_2\text{NaY}_{1-x}\text{Er}_x\text{F}_6$ ($x = 0.01$) at 4.2 K. PL excitation schemes are shown at the left.

populated from the $^4I_{11/2}$ level. In order to check the lifetime assignments, the TR PL from the $^4I_{13/2}$ level has also been recorded after excitation to the second excited state (trace (c)). Essentially the same kinetics as for excitation to the $^2H_{11/2}$ level are observed. In this way we rule out the possibility that the measured decay time of the $^4I_{11/2} \rightarrow ^4I_{15/2}$ transition would correspond to the lifetime of some intermediate long living state in the decay path from the $^2H_{11/2}$ level. Thus, it is demonstrated that transitions between the second and first excited states of Er^{3+} take place in these crystals and the long lifetimes of the levels involved indicate that they occur to large extent by radiative decay.

In order to examine possible quenching mechanisms for this luminescence, the lifetime of the $^4I_{11/2}$ level has also been measured at room temperature and for other Er^{3+} concentrations. The results, summarized in Table I, show that temperature only has a minor effect on the $2.7 \mu\text{m}$ luminescence. In contrast, at high Er-concentrations an important quenching of the $^4I_{11/2}$ lifetime is observed, most probably as a result of interactions (cross-relaxation, upconversion) between Er^{3+} ions.

Figure 2 presents PL transients for a 1 % Er^{3+} -doped GaN sample at 20 K. These signals have a more complicated time-dependence than those for the insulating material. All traces show an initial, as yet unexplained, fast component with a decay time in the sub-microsecond range, which will not be further considered here. A second fast component, observed in the traces after excitation to the $^2H_{11/2}$ level ((a) and (b)) with a decay time of $\sim 3 \mu\text{s}$, is most probably related to

Table I : Lifetime (in ms) of the $\text{Er}^{3+} ^4I_{11/2}$ level in $\text{Cs}_2\text{NaY}_{1-x}\text{Er}_x\text{F}_6$ at 4.2 K and room temperature. The error in the last digit is indicated as a subscript.

x	4.2 K	300 K
0.001	21 ₃	9 ₂
0.01	21 ₃	12 ₂
0.1	1.4 ₂	1.1 ₂
1	1.1 ₂	0.7 ₂

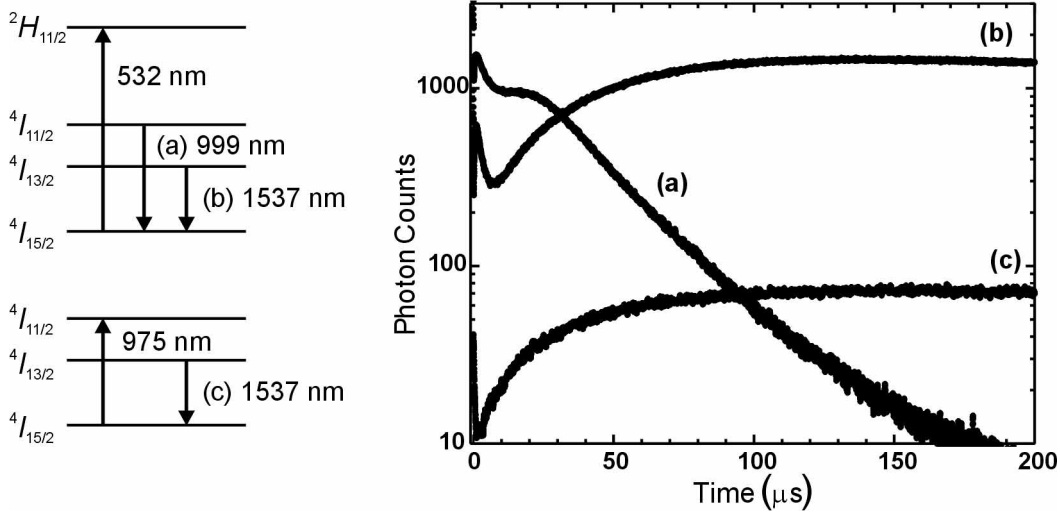


Figure 2 : Time resolved PL of the transitions from the second and first excited states of Er^{3+} in GaN (1 at. % doping concentration) at 20 K. PL excitation schemes are shown at the left.

visible green emission (${}^4S_{3/2} \rightarrow {}^4I_{15/2}$). The slow components hereafter do not exhibit single first order decay kinetics, as described by eq. (1). This is most probably a result of the formation of multiple Er^{3+} centers in these samples, as earlier reported for similarly grown structures [10]. The TR PL corresponding to the ${}^4I_{11/2} \rightarrow {}^4I_{15/2}$ transition (trace (a)) has a rise time of 7 – 10 μs and a decay time of 20 – 40 μs . The sum of these time constants roughly corresponds to the rise time of the ${}^4I_{13/2} \rightarrow {}^4I_{15/2}$ transition (30 – 50 μs , trace(b)). After direct excitation to the ${}^4I_{11/2}$ level, the latter transition has a rise time in the 30 – 40 μs range (trace(c)). These results thus show that the lifetime of the second excited state of Er^{3+} in this sample is 20 – 40 μs and the cumulative lifetime of the intermediate levels (${}^2H_{11/2} \rightarrow {}^4I_{11/2}$) amounts to 7 – 10 μs . The lifetime of the first excited state is found in the 1 – 1.5 ms range. In addition, it is demonstrated that the population of the ${}^4I_{13/2}$ level is dominated by transitions from the second excited state. At room temperature, the lifetime of the ${}^4I_{11/2}$ level is found to be $\sim 18 \mu\text{s}$. Again, no dramatic temperature quenching is observed for this transition.

As 2.7 μm emission from GaN: Er^{3+} is envisaged, it still has to be demonstrated that radiative transitions between the ${}^4I_{11/2}$ and the ${}^4I_{13/2}$ levels take place. Comparing the results for GaN with those for Cs_2NaYF_6 at low Er concentration, we find that the rise time of the ${}^4I_{11/2} \rightarrow {}^4I_{15/2}$ transition and the lifetime of the ${}^4I_{13/2}$ level are ~ 70 times shorter. The lifetime of the second excited state of Er^{3+} , however, appears to be shortened by an additional factor of ~ 8 , pointing to some nonradiative decay mechanism. One might consider multi-phonon relaxation between the ${}^4I_{11/2}$ and the ${}^4I_{13/2}$ level, which would imply that practically no radiative transitions between these levels occur. As only 5 longitudinal optical (LO) lattice phonons ($\hbar\Omega \sim 90 \text{ meV}$ [11]) are required to bridge the gap between the second and first excited state, multi-phonon relaxation may indeed be important [12]. This would, however, further imply that the lifetimes of the ${}^4S_{3/2}$ and ${}^4F_{9/2}$ levels experience an even stronger nonradiative quenching, as for these levels multi-phonon relaxation to the next state only requires 4 LO phonons. The rise time observed for the ${}^4I_{11/2} \rightarrow {}^4I_{15/2}$ transition and the occurrence of visible luminescence from these higher excited states (see e.g. [10]) do not support such a quenching mechanism. In fact, observations of

phonon replicas in the PL of GaN:Er³⁺ rather suggest coupling to the transverse optical (TO) phonon mode ($\hbar\Omega \sim 68$ meV) with a very small coupling strength ($S = 0.02$) [10] or to a local vibrational mode (14 meV) [13]. In either case, multi-phonon relaxation is not expected to dominate the $^4I_{11/2} \rightarrow ^4I_{13/2}$ transition. On the other hand, the doping level of the GaN sample is comparable to that of the Cs₂NaY_{0.9}Er_{0.1}F₆ crystal, for which an important concentration quenching of the $^4I_{11/2}$ lifetime is seen. We therefore we believe that the 2.7 μm emission from the GaN sample is also strongly quenched by interactions between Er³⁺ ions, which are possibly related with the appearance of visible (green, red) luminescence as well. Further experiments on GaN crystals with lower Er-concentrations are being undertaken in order to verify these hypotheses.

CONCLUSIONS

From time-resolved photoluminescence measurements in the near IR for a Cs₂NaY_{1-x}Er_xF₆ concentration series and for a 1 at. % Er³⁺-doped GaN sample, we have determined the lifetime of the second excited state of the Er³⁺ ion and shown that the first excited state is populated through $^4I_{11/2} \rightarrow ^4I_{13/2}$ transitions. It is argued that the latter transitions are not governed by multi-phonon relaxation. Hence, it is demonstrated that these materials should exhibit 2.7 μm emission, which is hardly quenched by temperature, but most likely shows an important concentration quenching. Realization of electrically driven MIR emission from Er-doped GaN, compatible with Si technology, thus seems feasible.

ACKNOWLEDGMENTS

This work was supported by the *US Army European Research Office*. H. Vrielinck acknowledges financial support from the *Fund for Scientific Research - Flanders (Belgium)*.

REFERENCES

1. E. Sorokin and I. T. Sorokina, *Appl. Phys. Lett.* **80** (18), 3289-3291 (2002).
2. S. D. Jackson and A. Lauto, *Laser Surg. Med.* **30** (3), 184-190 (2002).
3. V. Y. Ivanov, M. Godlewski, A. Szczerbakow, A. Omel'Chuk, A. Davydov, N. Zhavoronkov, and G. Raciukaitis, *Acta Phys. Pol.* **A 105** (6), 553-558 (2004).
4. M. Pollnau and S. D. Jackson, *Top. Appl. Phys.* **89**, 219-253 (2003).
5. A. J. Steckl, J. C. Heikenfeld, D. S. Lee, M. J. Garter, C. C. Baker, Y. Q. Wang, and R. Jones, *IEEE J. Sel. Top. Quant.* **8** (4), 749-766 (2002).
6. H. Q. Wu, C. B. Poitras, M. Lipson, J. Hunting and F. J. DiSalvo, *Appl. Phys. Lett.* **86** (19), art. no. 191918 (2005).
7. P. A. Tanner, Y. L. Liu, N. M. Edelstein, K. M. Murdoch, and N. M. Khaidukov, *J. Phys. Condens. Matter* **9** (37), 7817-7836 (1997).
8. J. R. G. Thorne, M. Jones, C. S. McCaw, K. M. Murdoch, R. G. Denning, and N. M. Khaidukov, *J. Phys. Condens. Matter* **11** (40), 7851-7866 (1999).
9. D. S. Lee, J. Heikenfeld, A. J. Steckl, U. Hommerich, J. T. Seo, A. Braud, and J. Zavada, *Appl. Phys. Lett.* **79**, 719-721 (2001).

10. V. Dierolf, C. Sandmann, J. Zavada, P. Chow, and B. Hertog, *J. Appl. Phys.* **95** (10), 5464-5470 (2004).
11. H. Siegle, G. Kaczmarczyk, L. Filippidis, A. P. Litvinchuk, A. Hoffmann, and C. Thomsen, *Phys. Rev. B* **55** (11), 7000-7004 (1997).
12. M. D. Shinn, W. A. Sibley, M. G. Drexhage, and R. N. Brown, *Phys. Rev. B* **27** (11), 6635-6648 (1983).
13. I. Izeddin, T. Gregorkiewicz, D. S. Lee, and A. J. Steckl, *Superlattice. Microstr.* **36**, 701-705 (2004).